ELSEVIER

Effect of Al–4Ti–5B master alloy on the grain refinement of AZ31 magnesium alloy

Yingxin Wang *, Xiaoqin Zeng, Wenjiang Ding

The State Key Laboratory of Matrix Composites, Shanghai Jiao Tong University, Huashan Road 1954, Shanghai 200030, PR China

Abstract

The effect of a new Al–4Ti–5B master alloy on the grain refinement of AZ31 magnesium alloy has been investigated. It is shown that grain refinement can be accomplished readily. Energy dispersive X-ray analysis and theoretical calculations show that TiB_2 particles act as the heterogeneous nuclei.
© 2005 Acta Materialia Inc. Published by Elsevier Ltd. All rights reserved.

1. Introduction

The use of magnesium alloys for structural components in the automotive and aerospace industries is attractive due to their high specific strength and low density. Increasing volumes of magnesium alloys are being used in the automotive industry to satisfy the demands for fuel efficiency and low emissions [1]. At present, magnesium components for structural applications are mainly produced by the high-pressure die casting process [2]. Compared with cast magnesium alloys, wrought magnesium alloys can be used to produce components with superior mechanical properties, which are attributed to the high quality of the billets before hot deformation. The finer grain size reduces the size of defects such as microporosity and second-phase particles, producing improved mechanical properties. Therefore, grain refinement is an important technique for improving the magnesium product quality. Meanwhile, grain refinement of a magnesium alloy is extremely effective in improving its formability at room temperature [3].

A variety of methods have been developed to refine magnesium–aluminum alloys, such as superheating, the Elfinal process, the addition of carbon, the agitation method, and adding particles (Al_4C_3, AlN, SiC, TiC) and solute elements (Sr, B, Ce, Nd, Y, La) [4–9]; of these methods, the addition of carbon-containing agents (CCl_6) offers practical advantages because of the low operating temperature involved and the less fading that results [10]. However, the problem encountered with this method is the emission of harmful chloride gas; also the chloride remaining in the magnesium alloys causes severe corrosion.

It is well known that Al–5Ti–B master alloy is an effective grain refiner in aluminum alloys [11], and it could also refine the ZA84 magnesium alloy, and TiB_2 particles were found to nucleate the α(Mg) grains [12]. However, due to the low boron content, there is a relatively small amount of TiB_2 particles present in the Al–5Ti–B master alloy. In this paper, the Ti to B atomic ratio is changed to improve the effectiveness of the master alloy and to eliminate the residual Ti so as to generate a larger amount of TiB_2 particles and produce a new Al–4Ti–5B master alloy. The effect of the new master alloy on the grain refinement of AZ31 magnesium alloy has been investigated.

2. Experimental procedure

The new Al–4Ti–5B master alloy was fabricated by adding KBF_4 and K_2TiF_6 to aluminum melt at about 1273 K using a graphite crucible in an intermediate frequency

---

* Corresponding author. Tel.: +86 21 6293 2239.
  E-mail address: wyx119@sjtu.edu.cn (Y. Wang).

Table 1
Chemical compositions of the Al–4Ti–5B master alloy (mass fraction %)

Master alloy	Ti	B	Al
Al–4Ti–5B	4.23	4.81	Bal.

Table 2
Chemical compositions of experimental alloys (mass fraction %)

Alloy no.	Al	Zn	Mn	Al–4Ti–5B	Mg
AZ31B	2.84	0.97	0.22	–	Bal.
AZ31-1	3.01	0.97	0.22	0.1	Bal.
AZ31-2	3.16	0.97	0.22	0.2	Bal.
AZ31-3	3.22	0.97	0.22	0.3	Bal.
AZ31-5	3.43	0.97	0.22	0.5	Bal.
AZ41	4.15	1.08	0.20	–	Bal.

induction-furnace. A commercial AZ31B magnesium alloy was melted in an electrical furnace using a mild steel crucible under a protecting gas ($0.3\%SF_6$ and $99.7\%CO_2$). Al–4Ti–5B master alloy was added into the melt at 750 °C. The melt was held for 30 min and then poured into a mild steel mold that was preheated to 200 °C with a size of 25 mm × 40 mm × 100 mm. The chemical compositions of the Al–4Ti–5B master alloy and the studied alloys are listed in Tables 1 and 2. AZ41 alloy was also prepared. Samples were sectioned from 15 mm near the edge of the ingots and heat treated in a sulfur atmosphere at 400 °C for 24 h followed by quenching in cold water in order to delineate the grain boundaries. Characterization of the grain size and qualitative analysis were conducted on selected specimens using a Leica MEF4M optical microscope (OM) and a JSM-5600LV scanning electron microscope (SEM) with an energy dispersive X-ray (EDX) spectrometer (Oxford Instruments). The mean linear intercept method was used to measure the average grain size.

3. Results

3.1. Characteristics of Al–4Ti–5B master alloy

Fig. 1 shows the XRD pattern of the new Al–4Ti–5B master alloy. There exist three phases, TiB_2, α-AlB_{12} and Al. The optical microstructure is illustrated in Fig. 2. Clusters of α-AlB_{12} particles are surrounded by a ring of TiB_2 particles and the particles outside the ring are mainly TiB_2. The size of the α-AlB_{12} particles is 5–10 μm and that of TiB_2 particles is 1–2 μm. The black spots are voids caused by particles torn out in the process of metallographic preparation.

3.2. Microstructures of the non-refined and refined AZ31 magnesium alloys

Fig. 3 shows the SEM image and EDX results of the refined AZ31-5 alloy. Many non-equilibrium eutectic phases (α-Mg + $Mg_{17}Al_{12}$) (marked by B, C, D, H, I and J) exhibiting a wide range of Al and Zn content are present in the interdendritic region. Zn-rich phases (marked by A, F and
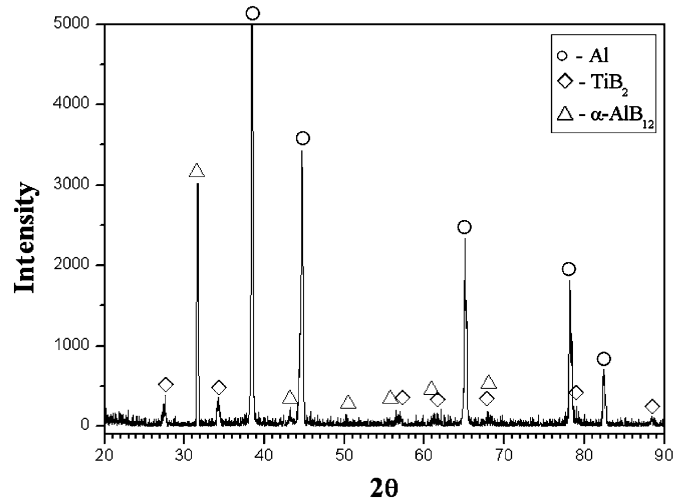

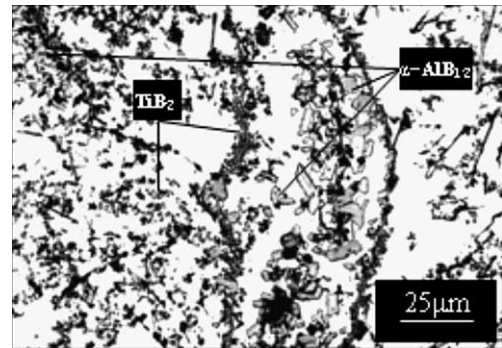Fig. 1. XRD diffraction pattern of the Al–4Ti–5B master alloy.

Fig. 2. Microstructure of the Al–4Ti–5B master alloy.

K) and Al–Mn phase (marked by L) are located in the α(Mg) matrix. It seems that there are no obvious differences in the shape and size of those particles in the refined alloy and those in the non-refined AZ31 magnesium alloy [13]. However, different Ti-containing particles (marked by E and G) appear. In the refined alloy, α-AlB_{12} particles and other B-containing particles are not found in the α(Mg) matrix.

Fig. 4 shows the optical microstructures of the heat-treated AZ31 magnesium alloy with different levels Al–4Ti–5B master alloy additions. AZ41 alloy acts as a reference. The grains can be refined dramatically by adding Al–4Ti–5B and the grain size of the AZ41 alloy is smaller than that of the AZ31 alloy. Fig. 5 demonstrates the dependence of actual average grain size on the amount of Al–4Ti–5B master alloy corresponding to Fig. 4, by using the mean linear intercept method. The average grain size of the non-refined AZ31 alloy is about 1100 μm and it decreases gradually with increasing Al–4Ti–5B. A minimum of 80 μm for the grain size can be obtained at an optimum level (0.3 wt.%), which is lower than that (1.0 wt.%) of the Al–5Ti–B master alloy [12]. The grain size increases somewhat with further addition of Al–4Ti–5B.
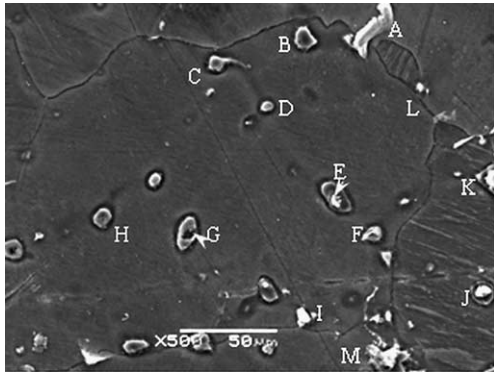
Fig. 3. SEM image and EDX results of the refined AZ31-5 alloy: A–M denote particles in the α-Mg matrix; B, C, D, H, I and J represent eutectic phases (α-Mg + $Mg_{17}Al_{12}$); A, F and K represent Zn-rich phases; L represents Al–Mn phase and E and G represent Ti-containing particles. EDX results are shown in the following table:

	Mg (at.%)	Al (at.%)	Zn (at.%)	Ti (at.%)	Mn (at.%)	Fe (at.%)
A	79.86	16.05	4.09	–	–	–
B	97.09	1.77	1.14	–	–	–
C	93.41	5.03	1.56	–	–	–
D	93.10	5.69	1.21	–	–	–
E	90.17	6.39	–	3.44	–	–
F	90.91	5.88	3.21	–	–	–
G	96.41	2.06	–	1.53	–	–
H	97.14	1.82	1.04	–	–	–
I	91.30	8.70	–	–	–	–
J	87.45	12.55	–	–	–	–
K	85.92	11.76	2.32			
L	36.14	50.71	–	–	13.15	–
M	42.51	42.28	2.15	–	4.31	8.75

4. Discussion

The effect of solute elements on the grain refinement is in controlling the growth of the nucleated grains and in subsequent nucleation, which has been investigated in various aluminum systems [14] and is explained in terms of the growth restriction factor (GRF). The constitutional undercooling generated by solute elements restricts grain growth by slowing diffusion of the alloying elements. Some alloying elements, such as Al, Zr, Sr, Si and Ca, have been reported to refine the pure magnesium obviously, because of the relatively larger GRF value [4]. Fig. 6 depicts the relationship between the grain size and the GRF value of Al. For different amounts of Al added to pure magnesium [4], the larger GRF value leads to a finer grain size up to a critical GRF value; the relationship of grain size and GRF value is in accordance with a sigmoid, which can be denoted by $Y_{grain\ size} = 587 + 887/(1 + \exp((x_{GRF} - 13)/3))$. It is presumed that the effect of Al in this work is similar to that in pure magnesium, that is, in this work, there is a sigmoidal relationship between the grain size and GRF value. The grain size is larger than that in Ref.
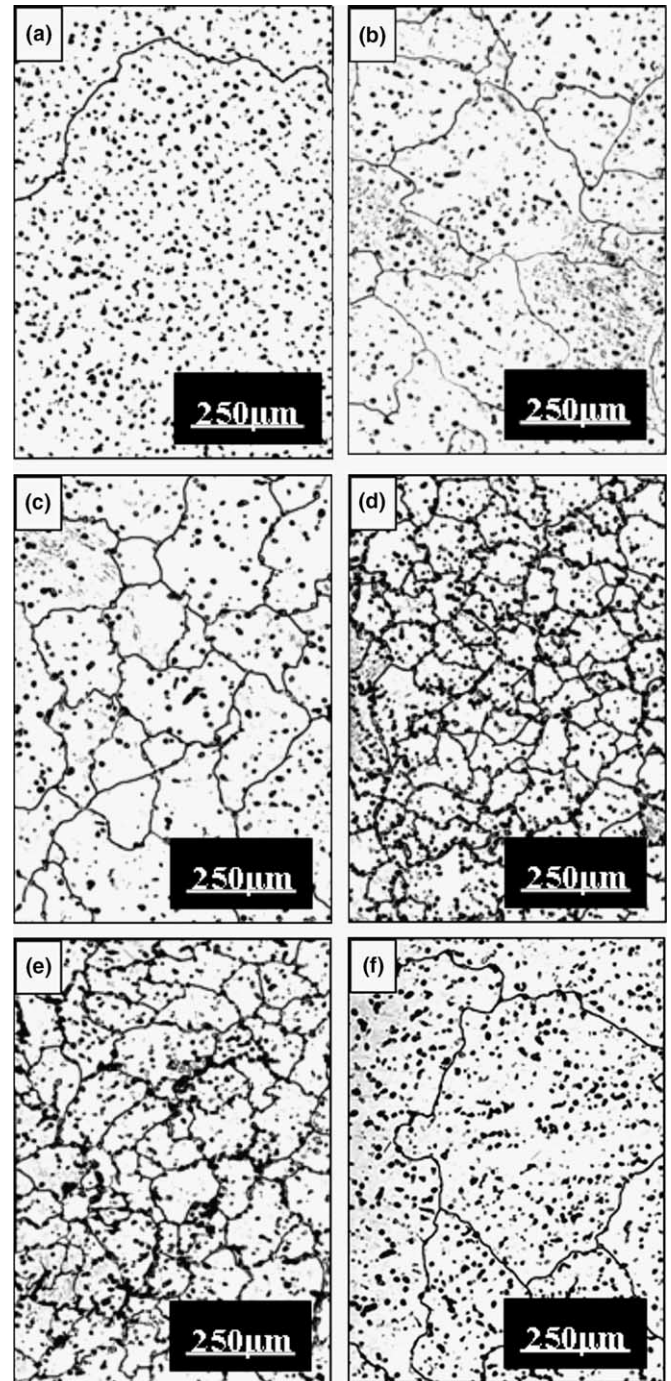

Fig. 4. Microstructures of heat-treated AZ31 alloy with different Al–4Ti–5B master alloy addition and AZ41 alloy: (a) without addition; (b) 0.1 wt.% addition; (c) 0.2 wt.% addition; (d) 0.3 wt.% addition; (e) 0.5 wt.% addition; (f) AZ41 alloy.

[4] because of the different cooling rate and Zn has no obvious effect on the grain refinement [15]. Parameter $m(k - 1)$ of Al in magnesium is 4.32 [4]. Therefore, the GRF value $(C_0m(k - 1))$ of Al in AZ31 alloy is 12.27 and that in AZ41 alloy is 17.93 in this work. The AZ31-5 alloy has the maximum extra Al that is added by the master alloy and the GRF value is 14.82. As can be seen from Fig. 6, the grain size of AZ31 alloy with extra Al up to 0.59 is
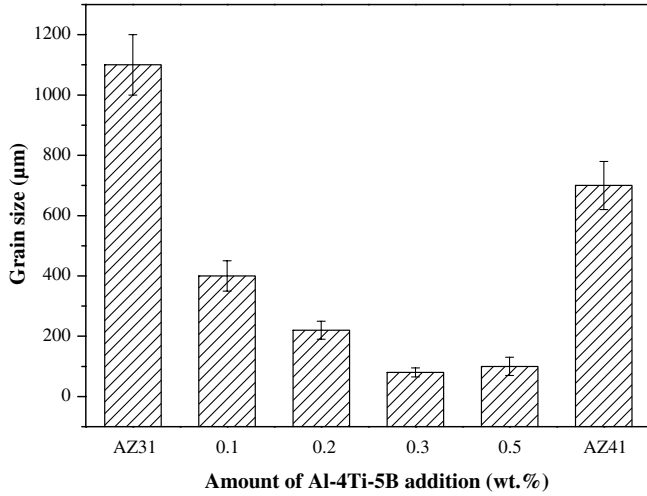
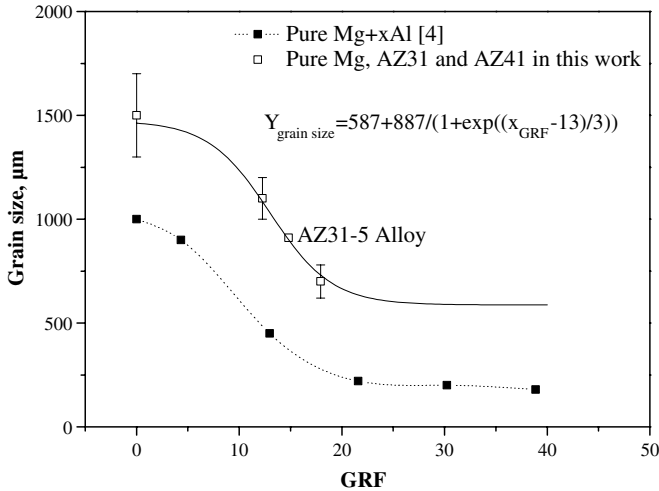Fig. 5. Dependence of grain size of the studied alloys on the addition of the master alloy and AZ41 alloy.

Fig. 6. Relationship between grain size and GRF value of Al.

about 950 μm. Hence, the extra Al is not likely to cause a significant change in grain size.

There is a necessary condition for the nucleant particles to act as heterogeneous nuclei, that is, the disregistry between low index planes of adjoining phases must be less than 15%. According to the disregistry model of two-dimensional lattices proposed by Bramfitt [16], the formula is

$$\delta_{(hkl)_n}^{(hkl)_s} = \sum_{i=1}^{3} \left\{ \left| d[uvw]_s^i \cos\theta - d[uvw]_n^i \right| / d[uvw]_n^i \right\} / 3 \times 100\%,$$

where $(hkl)_s$ and $(hkl)_n$ are the low index planes of the matrix and nucleus, respectively, $[uvw]_s$ and $[uvw]_n$ are the low index orientations in $(hkl)_s$ and $(hkl)_n$, respectively, $d[uvw]_s$ and $d[uvw]_n$ are atomic spacing distances along $[uvw]$, and θ is the angle between $[uvw]_s$ and $[uvw]_n$. The Al–4Ti–5B master alloy has two particles, TiB_2 and α-AlB_{12}, which are stable in molten magnesium alloy because of their high melting point. The structure of the TiB_2 phase is hexagonal and the lattice constants are $a = 0.3028$ nm and $c = 0.3228$ nm [17], and the structure of α-AlB_{12} phase is tetragonal and the lattice constants are $a = 1.016$ nm and $c = 1.428$ nm [18]. The structure of Mg is hexagonal and the lattice constants are $a = 0.321$ nm and $c = 0.521$ nm [15]. The disregistries of possible crystallographic orientation relationships between TiB_2, α-AlB_{12} and α-Mg matrix are listed in Tables 3 and 4. The disregistry between α-AlB_{12} and α-Mg matrix is far larger than 15% in the two low index planes which shows α-AlB_{12} particles are not good heterogeneous nuclei. Nishino et al. [8] have also shown that α-AlB_{12} particles are not effective grain nuclei to the AZ91 magnesium alloy. In addition, very few α-AlB_{12} particles are observed in the AZ31 alloy as shown in Fig. 3. It is therefore probable the α-AlB_{12} particles settle to the bottom of the crucible. The smallest disregistry between TiB_2 and α-Mg is 5.6% while their crystallographic

Table 3
The disregistry of possible crystallographic orientation relationships between TiB_2 and α-Mg matrix

	$(0001)_{TiB_2} \| (0001)_{Mg}$			$(0001)_{TiB_2} \| (10\bar{1}0)_{Mg}$		
$[uvw]_{TiB_2}$	[100]	[110]	[010]	[$\bar{2}$10]	[010]	[$\bar{1}$00]
$[uvw]_{Mg}$	[100]	[110]	[010]	[001]	[010]	[011]
$d[uvw]_{TiB_2}$	0.303	0.303	0.303	0.525	0.303	0.303
$d[uvw]_{Mg}$	0.321	0.321	0.321	0.521	0.321	0.612
θ	0	0	0	0	0	1.64
δ		5.6%			18.96%	

Table 4
The disregistries of possible crystallographic orientation relationships between α-AlB_{12} and α-Mg matrix

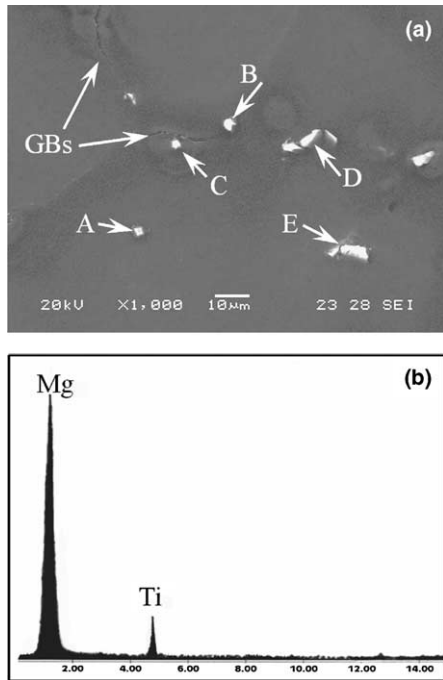|	$(001)_{AlB_{12}} \| (001)_{Mg}$			$(001)_{AlB_{12}} \| (210)_{Mg}$		
$[uvw]_{AlB_{12}}$	[001]	[010]	[011]	[001]	[010]	[011]
$[uvw]_{Mg}$	[010]	[$\bar{2}$10]	[$\bar{1}$00]	[010]	[001]	[011]
$d[uvw]_{AlB_{12}}$	1.016	1.016	1.436	1.016	1.016	1.436
$d[uvw]_{Mg}$	0.321	0.556	0.321	0.521	0.321	0.612
θ	0	0	15	0	0	13.36
δ		210.4%			146.6%	

Fig. 7. SEM image and EDX analysis of the AZ31-3 alloy: (a) SEM morphology; (b) EDX of particle A (A–E denote particles in the α-Mg matrix, GBs refers to the grain boundaries). EDX results are shown in the following table:

	Mg (at.%)	Al (at.%)	Zn (at.%)	Ti (at.%)
A	94.59	–	–	5.41
B	65.31	33.88	0.81	–
C	74.49	25.51	–	–
D	76.49	21.32	2.19	–
E	78.22	19.76	2.02	–

orientation relationship is $(0001)_{TiB_2} \| (0001)_{Mg}$. Hence, TiB_2 particles can act as the heterogeneous nuclei for the grain refinement of AZ31 magnesium alloy.

Fig. 7 shows an SEM image and EDX analysis of the AZ31-3 alloy. In the central part of the grain, there exist two types of particles, particle E is eutectic phase and a Ti-containing particle A. The former particle is not heterogeneous nucleus in magnesium alloys [19]. Therefore, Ti-containing particles A maybe nucleate the α-Mg grain. Wang et al. [20] shows that there is no reaction between TiB_2 particles and the Mg matrix. Hence, particle A is not a single Mg–Ti phase, but TiB_2 particle (no B element maybe caused by the low resolution capacity of EDX analysis). During the solidification of AZ31 magnesium alloy, Al solute elements segregate in front of the growing interface and generate constitutional undercooling, which is same effect as for the Ti element in the aluminum alloy [21]. Hence, TiB_2 particles activated by constitutional undercooling act as the heterogeneous nuclei to nucleate the α-Mg grains.

5. Conclusions

The effect of a new Al–4Ti–5B master alloy on the grain refinement of AZ31 magnesium alloy has been investigated. It is shown that the grain size of AZ31 magnesium alloy can be effectively reduced from 1100 μm to about 80 μm by the optimum addition lever of 0.3 wt.% Al–4Ti–5B master alloy. SEM observation, EDX result and theoretical calculation show that TiB_2 particles act as heterogeneous nuclei.

References

[1] Ravi Kumar NV, Blandin JJ, Desrayaud C, Montheillet F, Suéry M. Mater Sci Eng A 2003;359:150.
[2] Fridrich H, Schumann S. J Mater Process Technol 2002;117:276.
[3] Chang TC, Wang JY, Lee O. J Mater Process Technol 2003;140:588.
[4] Lee YC, Dahle AK, St John DH. Metall Mater Trans A 2000;31: 2895.
[5] Lee YC, Dahle AK, St John DH. In: Kaplan HI, Hryn JN, Clow BB, editors. Magnesium Technology 2000. Warrendale (PA): TMS; 2000. p. 211.
[6] Dahle AK, Lee YC, Nave MD, Schaffer PL, St John DH. J Light Met 2001;1:61.
[7] Luo A. Can Metall Quart 1996;35(4):375.
[8] Nishino N, Kawahara H, Shimizu Y, Iwahori H. In: Kainer KU, editor. Proceedings of international congress "magnesium alloys and their applications", Munich, Germany; 2000. p. 59.
[9] Cao P, Qian M, St John DH. Scripta Mater 2004;51:125.
[10] Jin QL, Eom JP, Lim SG, Park WW, You BS. Scripta Mater 2003;49: 1129.
[11] Greer AL, Bunn AM, Tronche A, Evans PV, Bristow DJ. Acta Mater 2000;48:2823.
[12] Wang YX. Master paper, Zhengzhou University; 2003.
[13] Wang YX, Zeng XQ, Ding WJ, Luo AA, Sachdev AK. In: Neelameggham NR, Kaplan HI, Powell BR, editors. Magnesium Technology 2005. Warrendale, PA: TMS; 2005. p. 85.
[14] Johnsson M, Bäckerud L. Z Metallkd 1996;87(3):216.
[15] ASM Specialty Handbook, Magnesium and magnesium alloys. Materials Park (OH): ASM International; 1999.
[16] Bramfitt BL. Metall Trans A 1970;1(7):1987.
[17] Ji JM, Zhou F, Li ZH. Chin J Nonferr Met 2000;10(3):358 [in Chinese].
[18] JCPDS: 12-0640.
[19] Nishino N, Kawahara H, Shimizu Y. US patent No. 6,395,224 B1.
[20] Wang H, Jiang QC, Zhao Y, Zhao F. J Alloys Compd 2004;379:L4.
[21] Easton M, St John DH. Metall Mater Trans A 1999;30:1625.